49th AIAA Aerospace Sciences Meeting including the New Horizons Forum and Aerospace Exposition
4 - 7 January 2011, Orlando, Florida
AIAA 2011-1256

Aerodynamic Analysis of Open Trailing Edge Airfoils at Low Reynolds Number

Rodolfo Sant[1], Luis Ayuso[2] and Jose Meseguer[3]
Universidad Politecnica de Madrid, 28040 Madrid, Spain

A study has been made on the influence of the open trailing edge in airfoils used in different devices relating their aerodynamic performances. Wind tunnel tests have been made at different Reynolds numbers and angles of attack in order to show this effect. Besides, a quantitative study of the aerodynamic properties has been made based on the different trailing edge thickness.

Nomenclature

C_L = lift coefficient
C_D = drag coefficient
C_M = pitch moment
C_P = pressure coefficient based on the free stream static and dynamics pressures
c = main chord length, m
Re = Reynolds number
α = angle of attack, degrees
TE = trailing edge thickness to chord ratio, % c

I. Introduction

The interest of this study is based on the observation of the effect that in some manufacturing processes of various vehicles wings, such as wind turbine blades or other devices that use aerodynamic profiles, produce open trailing edge, with bigger thickness than original airfoil, because they are manufactured in two parts, top surface and bottom surface and subsequently joined. In this last step it might appear a small thickness gain on the trailing edge. Normally these imperfections are corrected through a refill and/or sanding processes using many hours of manual labor.

Therefore the initial objective of this research is to determine the level of influence, in the aerodynamic characteristics at low Reynolds numbers [1-6], of these imperfections in the manufacture, and determine whether there may be a value for which it would not be necessary to correct them. Previous studies on simply truncated trailing edge to achieve the required trailing edge thickness [8,11], or adding thickness to either side of the chamber line [12,13] exhibits increased maximum lift but increased minimum drag also.

II. Experimental Setup

The experiments were performed in an open-circuit low-speed blow up wind tunnel located in the Aerodynamics Laboratory managed by Aerotecnia Department at the Universidad Politecnica de Madrid. The wind tunnel has a test section with a 1.2 by 0.16 m cross section and several windows, including an optically transparent one (Fig. 1). The wind tunnel has a contraction section upstream of the test section, with screen structures to provide uniform low-turbulent incoming flow to enter into the test section. Velocity dispersion is less than 1% outside boundary layer and

[1] Professor, Department of Aerotecnia/UPM, rodolfo.sant@upm.es, AIAA Senior Member.
[2] Professor, Department of Aerotecnia/UPM, luis.ayuso@upm.es, AIAA Senior Member.
[3] Principal Research Scientist, IDR/UPM, j.meseguer@upm.es.

the mean turbulence level is les than 0.5%. The air speed in test section can be steadily regulated for values from 5 to 30 m/s and therefore test the airfoils up to 500,000 Reynolds numbers.

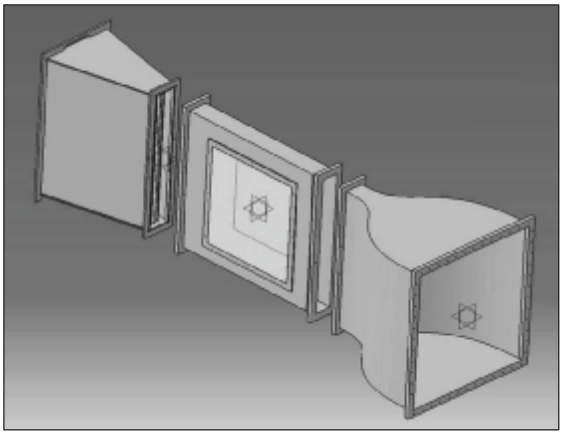

Figure 1. Wind tunnel scheme. *Contraction, test-section and diffuser configuration.*

The airfoil used in the present study is a NACA0012 airfoil [7]. Two models have been built for the tests, one of them used for forces measurement with an electronic forces balance and for the use with laser anemometry. The other model is also provided with 34 pressure taps at its median span (Fig. 2). Both models have been manufactured in a numerical control milling machine using chemical wood, with great stability and a good surface finish, and they are provided with a mechanism that allows opening the trailing edge.

Model span is 15.8 cm, whereas that of the wind tunnel test chamber wide is 16 cm. No special provision has been made to avoid the gap between model and wind tunnel walls, nor to correct measure results to take into account this effect[14], have been undertaken. It must be emphasized that the aim of this work is to compare the aerodynamic effect of different airfoil trailing edge thicknesses.

The models have a 24 cm chord, allowing test up to 450,000 Reynolds number with 30 m/s air velocity in the test section.

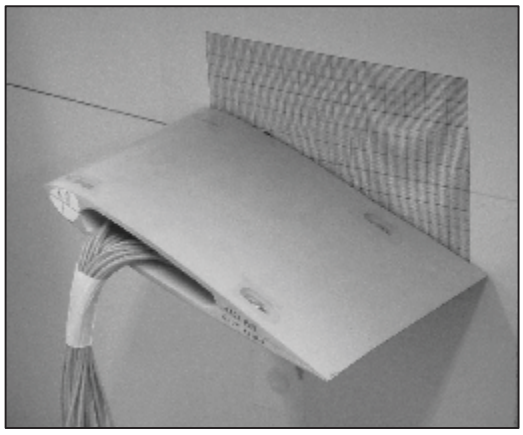

Figure 2. NACA 0012 model. *Airfoil model fitted with pressure taps.*

The forces have been measured through a 3 component electronic forces balance of PLINT Company, located on one of the side walls of the test camera, which allows to measure lift and drag forces, and pitch moment.

The pressure taps were connected to a pressure acquisition system (DSA3217, Scanivalve Corp.) for surface-pressure measurements.

Models have been tested from -2º to 22° angles of attack, and Re = 75,000; 150,000; 300,000 and 450,000.

For this study, both parts, upper and lower part, are able to be rotated around the leading edge using different gauges, in order to obtain the trailing edge thickness necessary, as shown in Figure 3, so a new airfoil is obtained, with a thicker trailing edge, as well as larger airfoil thickness and different location of this maximum thickness. The trailing edges tested were of 2%, 4%, 6%, 8% and 10% of main chord length.

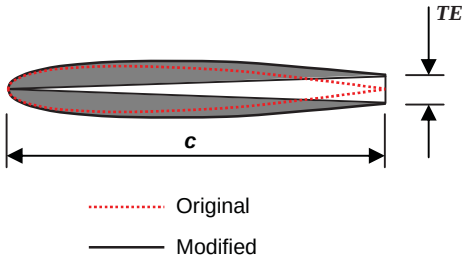

Figure 3. Trailing edge thickness. *Upper and lower parts are able to be rotated around the leading edge to obtain the trailing edge thickness necessary.*

In all cases the following measures were made:

- Lift coefficient C_L and drag coefficient C_D, through the three components forces balance.
- Upper and lower surface pressure with scanivalve.

III. Experimental Results

The experimental results are presented in the form of C_L and C_D versus angle of attack, and C_L/C_D ratio versus angle of attack.

The original airfoil, NACA0012, at Reynolds numbers studied presents an increment in maximum lift coefficient as Reynolds number increase, as well as a change in the kind of stall, from smooth stall at lower *Re*, to sharp stall at higher *Re* studied[15], as shown in fig. 4 and 5.

Experiments show that at same Reynolds number the small values of trailing edge thickness causes an increase in the maximum C_L [9,11,12,13], for higher values of trailing edge thickness the trend is to have a limit in this maximum C_L values[12,9]. At a fixed Reynolds number the minimum C_D increases as the size of the trailing edge thickness increases[9,12,13]. This increase in drag coefficient with the trailing edge thickness is bigger as the Reynolds number increases[9,13]. Looking at the variation of C_D with *Re* at a fixed trailing edge thickness shows that C_D decreases for all thicknesses as the Reynolds number increases[8,12].

Figures 4 and 5 show the effect of the trailing edge thickness size on the lift coefficient at a fixed Reynolds number of 75,000; 150,000; 300,000 and 450,000; and their influence on maximum C_L values as well as the slope of the linear part.

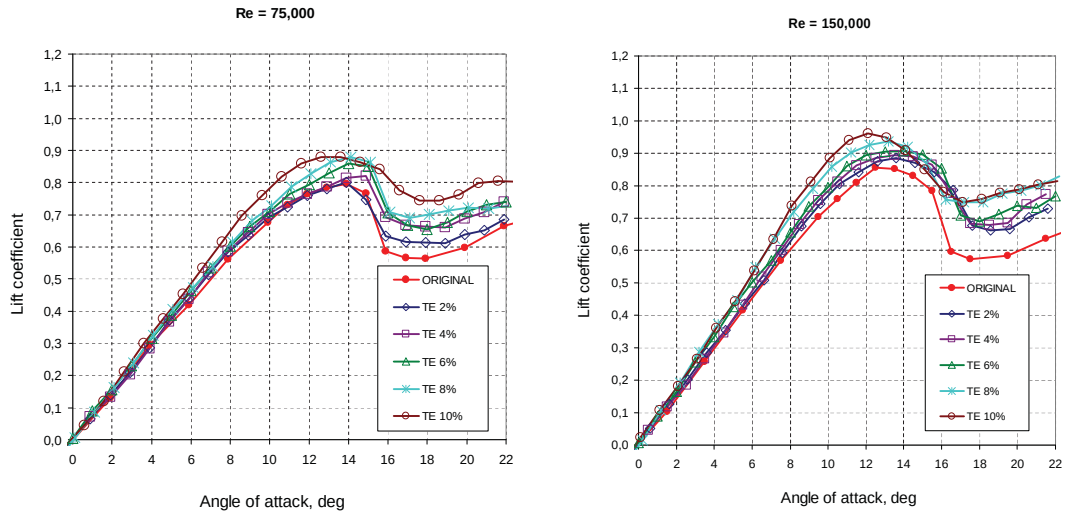

Figure 4. Lift coefficient versus angle of attack. *Re = 75,000 and 150,000. Effect of trailing edge thickness.*

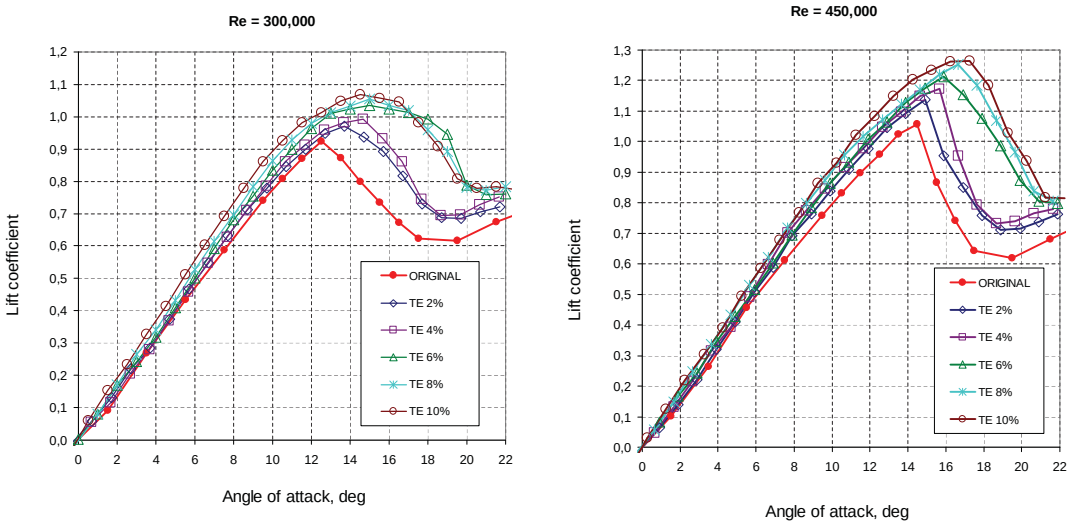

Figure 5. Lift coefficient versus angle of attack. *Re = 300,000 and 450,000. Effect of trailing edge thickness.*

It must be pointed out that, irrespective of the value of the Reynolds number, increasing of trailing edge thickness produces a significant growth of the lift coefficient, including the maximum lift coefficient (for trailing edge thickness of 10% the maximum lift coefficient growth between 10% and around 20%). This growth of the lift coefficient is bigger as the Reynolds number increases. Due to the fact that the lift coefficient is bigger at each angle of attack, the slope of the liner part increases as the trailing edge increases (until around 15% at the maximum thickness studied), this effect rises for bigger *Re*. For the smaller *Re* studied, the angle of attack for the maximum lift are similar for all trailing edge thicknesses studied, but for the bigger *Re* studied, the angle of attack for the maximum lift increases with de trailing edge thickness as well as the kind of stall change from smooth to sharp.

On the other hand the increase of trailing edge thickness produces a noticeable growth of the drag coefficient, including de minimum drag, especially strong at the biggest *Re* studied (for trailing edge thickness of 10% the minimum drag coefficient growth more than 100%). Figures 6 and 7 show the effect of the trailing edge thickness

size on the drag coefficient at 75,000; 150,000; 300,000 and 450,000 Reynolds number and their influence in C_D values along the angle of attack range.

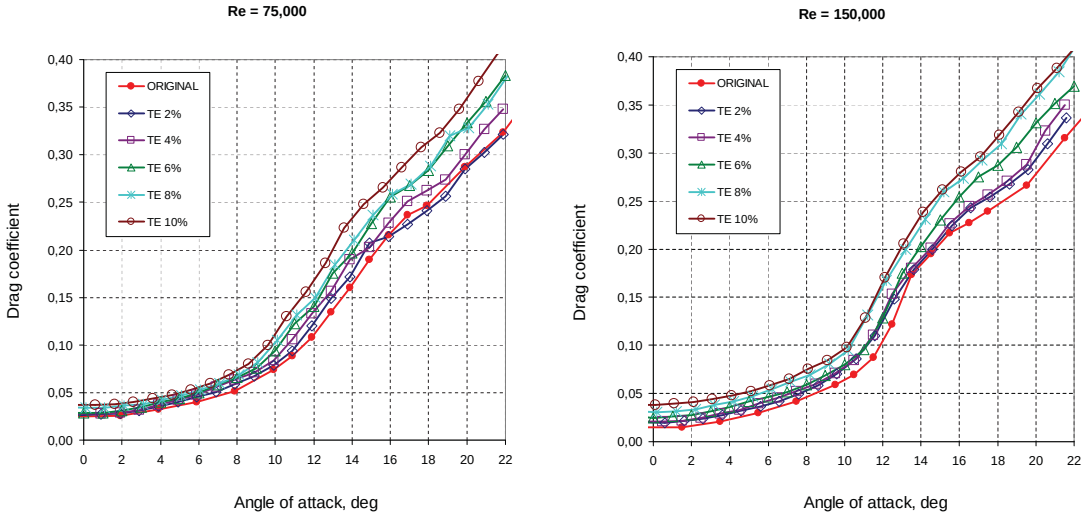

Figure 6. Drag coefficient versus angle of attack. *Re = 75,000 and 150,000. Effect of trailing edge thickness*.

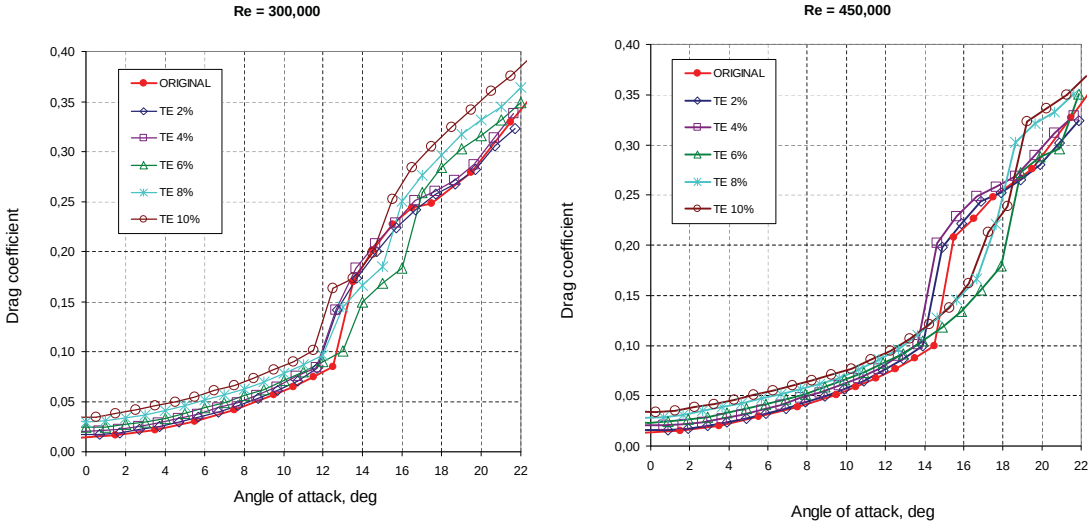

Figure 7. Drag coefficient versus angle of attack. *Re = 300,000 and 450,000. Effect of trailing edge thickness*.

Figures 8 and 9 show the effect of the trailing edge thickness size on the lift to drag ratio at 75,000; 150,000; 300,000 and 450,000 Reynolds number and their influence in C_D versus angle of attack range.

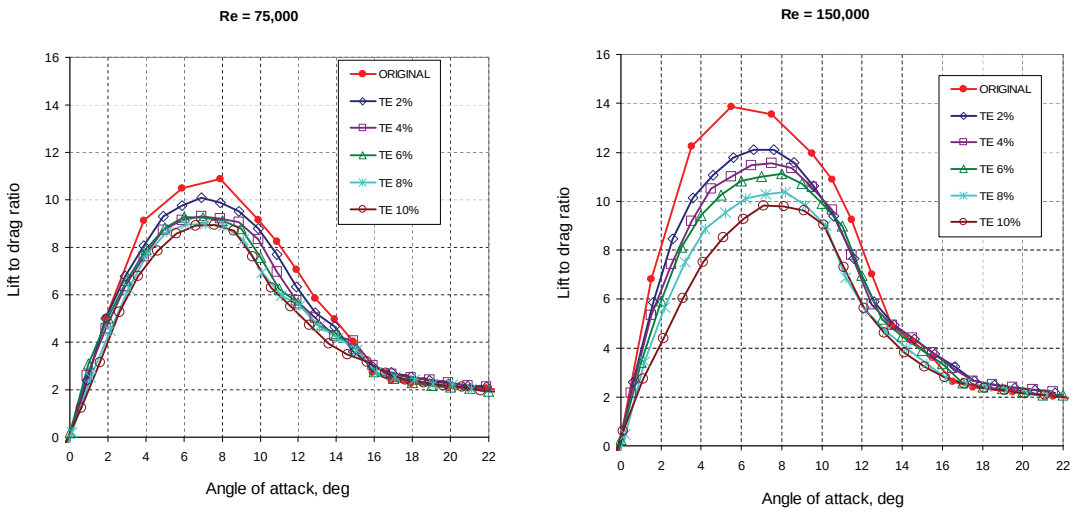

Figure 8. Lift to drag ratio versus angle of attack. *Re = 75,000 and 150,000. Effect of trailing edge thickness.*

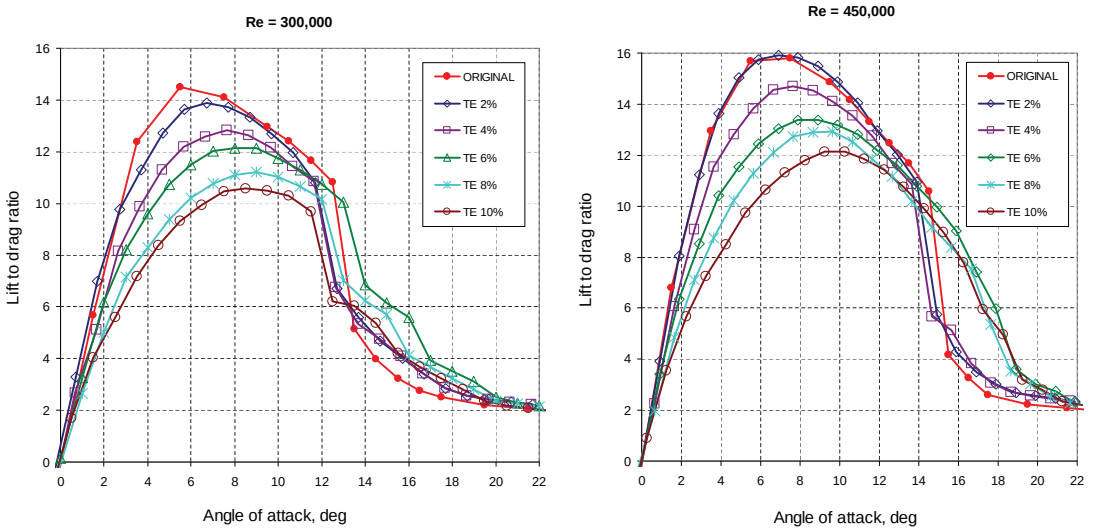

Figure 9. Lift to drag ratio versus angle of attack. *Re = 300,000 and 450,000. Effect of trailing edge thickness*.

Due to the fact that the drag coefficient increases more than the lift coefficient, the lift to drag ratio decreases at all angles of attack and at all *Re* studied, including its maximum value (for trailing edge thickness of 10% the maximum lift to drag ratio decreases between 15% at lowest *Re* studied and around 30% for the highest *Re* studied). At the same time, the angles of attack for the maximum C_L/C_D are similar for the lowest *Re* studied independently of the trailing edge thickness, while when the *Re* is bigger this angle of attack for the maximum C_L/C_D increases significantly with the trailing edge thickness.

Those experiments carried out with pressure taps show a short laminar bubble. After laminar boundary layer separates from the airfoil surface, the flow can reattach to the surface as a turbulent shear layer. This region between the laminar separation and the reattachment is called a laminar separation bubble [9]. The laminar separation bubble on the airfoil is classified into a short bubble and a long bubble. With increasing angle of attack, the chordwise length of the short bubble shortens and its position moves toward the leading edge. With further increase in the

angle of attack, the short bubble fails to reattach on the airfoil surface, what is known as a short bubble burst and this bubble burst causes the airfoil stall. The long bubble, which is formed after the burst, increases its chordwise length as the angle of attack is increased beyond the stall angle. The stall characteristics of the airfoil are strongly dependent upon these two types of bubbles. The negative pressure peak near the leading edge is observed when the short bubble is formed. When the long bubble is formed after the bubble burst, this negative pressure peak is destroyed and a relatively flattened pressure distribution is formed (Fig. 10). Early investigations of the short bubble mainly focused on predicting the short bubble burst [9–11]. Although the precise prediction of the short bubble burst has not been accomplished, it was revealed that the laminar transition and turbulent flow inside the short bubble play an important role in determining the short bubble burst.

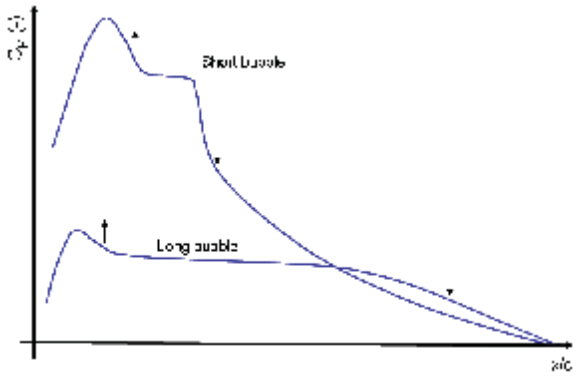

Figure 10. Pressure coefficient in laminar separation bubble.
Separation and reattachment of short and long bubbles.

For the lowest Reynolds number studied, Re=75x10^3, pressure distributions along the airfoil chord for the nominal airfoil case and several trailing edge studied are shown in Fig. 11 (these distributions correspond to angles of attack close to the stalling angle). These plots suggest that the laminar burble after the suction peak is growing as the angle of attack increases, independently of the trailing edge thickness, so the stall is smooth.

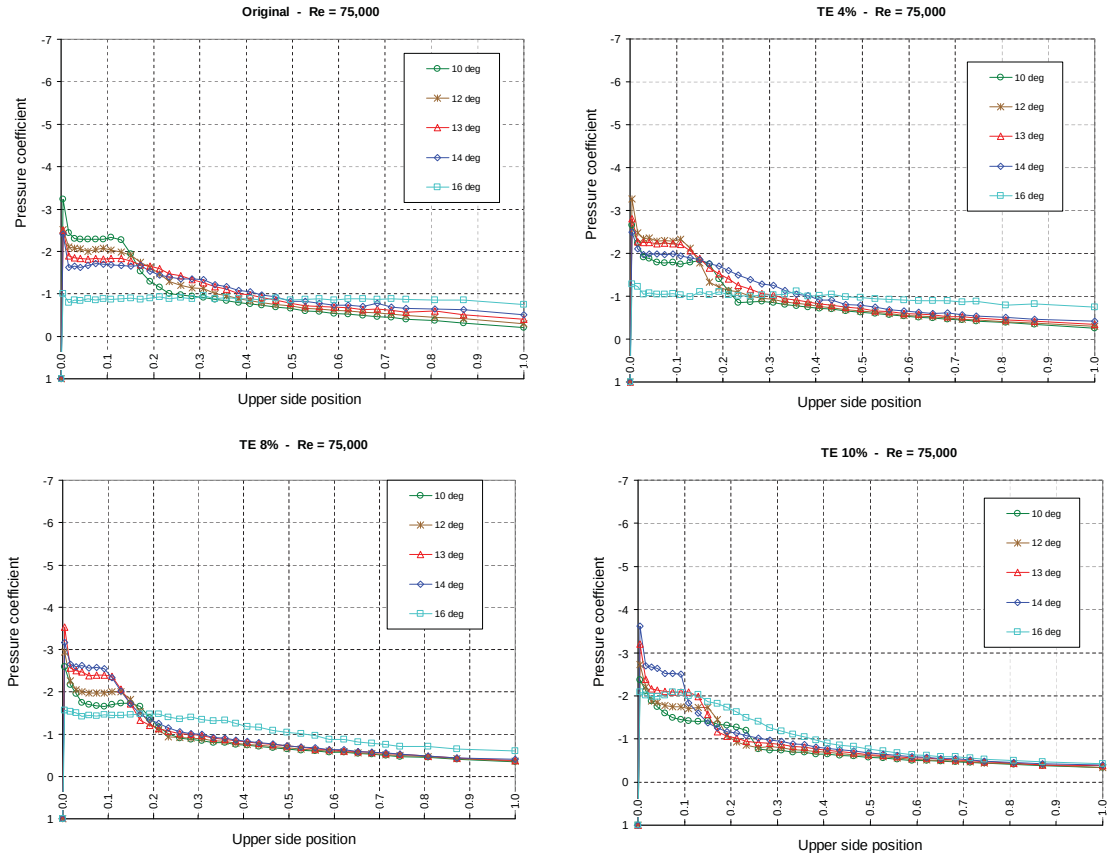

Figure 11. Pressure coefficient. *Cp distribution along the upper side, Re=75,000 and angles of attack close to the stalling angle.*

For Reynolds number $150x10^3$, pressure distributions along the airfoil chord for the nominal airfoil case and several trailing edges studied are shown in Fig. 12. According with these plots the behaviour is similar to *Re*=$75x10^3$, so the stall is smooth too, independently of the trailing edge thickness.

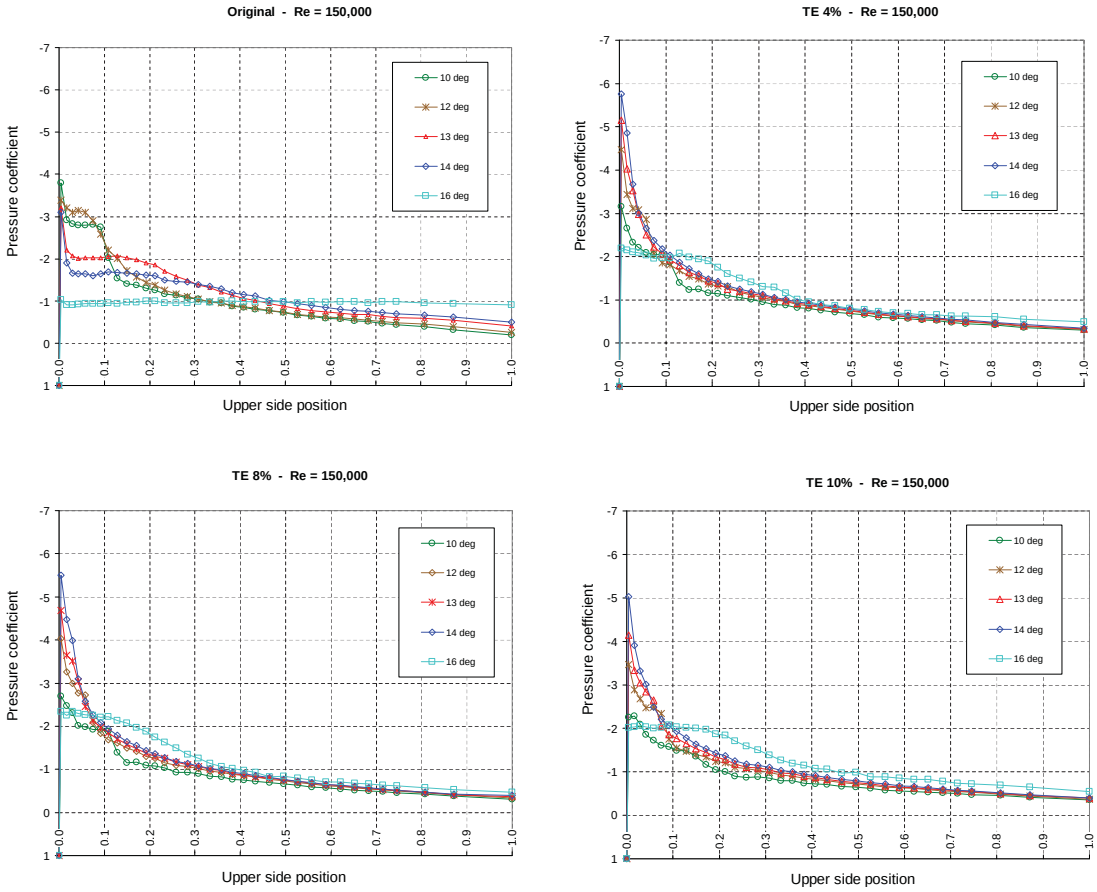

Figure 12. Pressure coefficient. *Cp distribution along the upper side, Re= 150,000 and angles of attack close to the stalling angle.*

However, for Reynolds number $300x10^3$ pressure distributions (Fig. 13) indicates that in the original profile a laminar recirculation bubble appears (see a high suction pressure near the leading edge followed by a plateau area and a sudden pressure recovery) that is shorter and closer to the leading edge as the angle of attack increases (the leading edge suction peak increasing accordingly) until the bubble shear layer can not reattach and the airfoil stalls suddenly (note that at • = 16º the boundary layer is separated on the whole airfoil upper surface). On the other hand, when the trailing edge thickness increases, this change and the laminar burble after the suction peak grows as the angle of attack increases, so the stall is smooth.

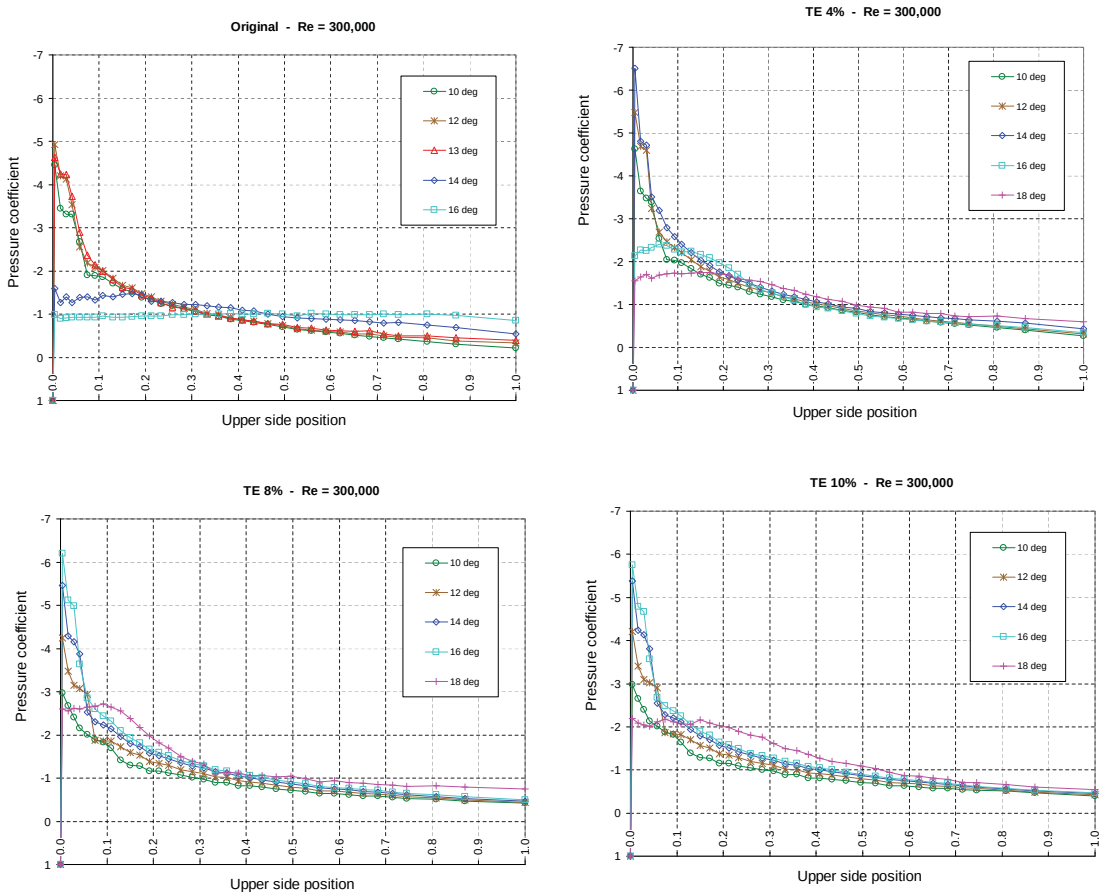

Figure 13. Pressure coefficient. *Cp distribution along the upper side, Re=300,000 and angles of attack close to the stalling angle.*

For the highest Reynolds number studied, *Re*=450x10^3, pressure distributions along the airfoil chord corresponding to angles of attack close to the stalling angle are shown in Fig. 14. These plots suggest that the behaviour is similar to Reynolds number 300x10^3, so sudden stall occurs for original airfoil and small trailing edge thickness while smooth stall appears when the trailing edge thickness increases.

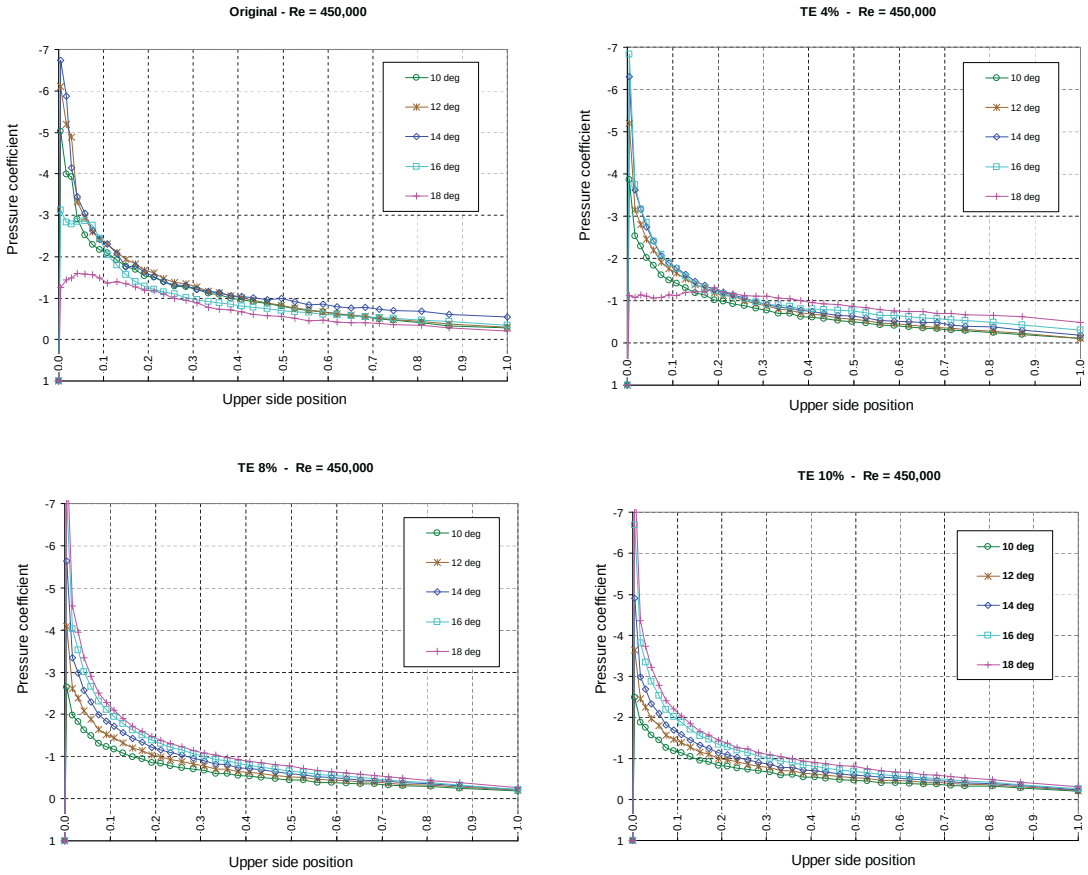

Figure 14. Pressure coefficient. *Cp distribution along the upper side, Re=450,000 and angles of attack close to the stalling angle.*

IV. Conclusion

Experiments shows a general increment of the lift coefficient as the trailing edge thickness increases, so the lift slope increases as well as the maximum lift coefficient (fig. 15), bigger as the Reynolds number increases.

On the other hand, a general increment of the drag coefficient, including the minimum drag (fig. 16) occurs. Due to the fact that the increment in drag is bigger than the increases of lift, the lift to drag ratio is smaller (fig. 17), especially for the biggest thickness studied and the maximum Reynolds number studied.

The results shows that a small size in thickness of open trailing edge could be tolerated, especially at the higher Reynolds number studied, with a small reduction in its aerodynamics efficiency as well as present an improvement in the lift coefficient.

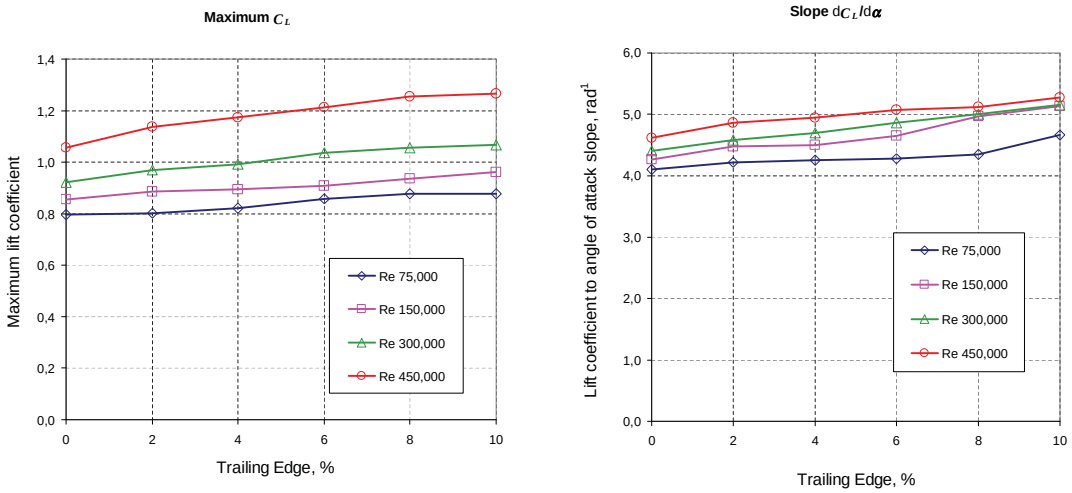

Figure 15. Maximum lift coefficient and lift coefficient slope. *Variation of maximum lift coefficient and lift coefficient slope versus trailing edge thickness in percentage.*

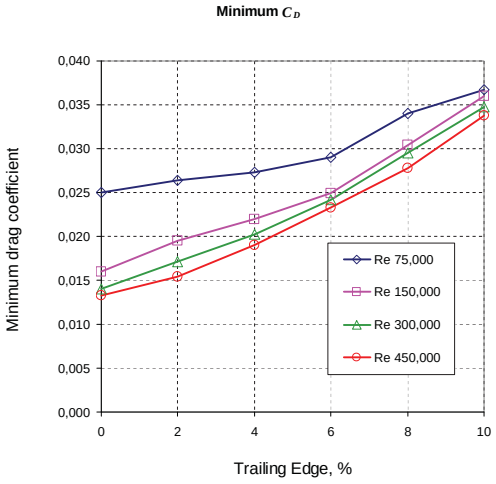

Figure 16. Minimum drag coefficient. *Variation of minimum drag coefficient versus trailing edge thickness in percentage.*

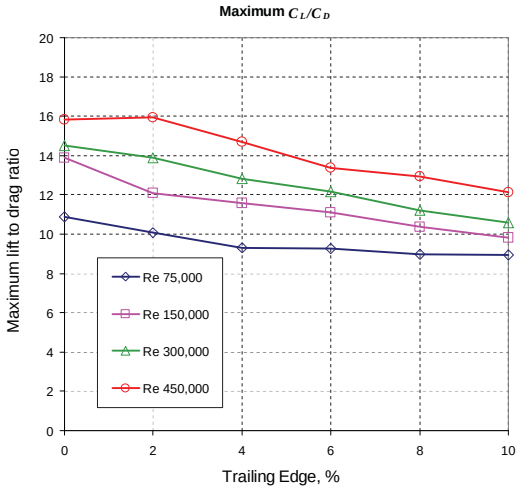

Figure 17. Maximum lift to drag ratio. *Variation of maximum lift to drag ratio versus trailing edge thickness in percentage.*

References

[1]Lissaman, P.B.S., "Low–Reynolds-Number Airfoils," *Annual Review of Fluid Mechanics*, Vol.15, Jan. 1983, pp. 223-239.

[2]Carmichael, B.H., "Low Reynolds Number Airfoil Survey," NASA CR-165803, Vol.1, Nov. 1981.

[3]Nagamatsu, H.T., and Cuche, D.E., "Low Reynolds Number Aerodynamics Characteristics of Low-Drag NACA 63-208 Airfoil," *Journal of Aircraft*, Vol.18, No.10, 1981, pp. 833—837.

[4]Schmitz, F.W., "Aerodynamik des Flugmodells," Verlag, Duisburg, Germany, 1957.

[5]Cebeci, T., "Essential Ingredients of a Method for Low Reynolds Number Airfoils," *AIAA Journal*, Vol.27, No.12, 1989, pp. 1680—1688.

[6]Mueller, T.J. and Batill, S.M., "Experimental Studies of Separation on a Two-Dimensional Airfoil at Low Reynolds Number," *AIAA Journal*, Vol.20, No.4, 1982, pp. 457—463.

[7]Abbott, I.H., and von Doenhoff, A.E., "Theory of Wing Sections," Dover, New York, 1959.

[8]Sato, J. and Sunada, Y., "Experimental Research on Blunt Trailing-Edge Airfoil Sections at Low Reynolds Number," *AIAA Journal*, Vol.33, No.11, 1995, pp.2001-2005.

[9]Standish, K.J., and van Dam, C.P., "Analysis of Blunt Trailing Edge Airfoils," *AIAA 41st Aerospace Sciences Meeting and Exhibit*, 2003.

[10]Standish, K.J., and van Dam, C.P., "Aerodynamic Analysis of Blunt Trailing Edge Airfoils," *Journal of Solar Energy Engineering*, Vol 125, Issue 4, pp 479-488, 2003. doi:10.1115/1.1629103.

[11]Ramjee, V., Tulapurkara, E.G., and Balabaskaran, V., "Experimental and Theoretical Study of Wings with Blunt Trailing Edge," *AIAA Journal of Aircraft* Vol. 23, NO, 4. April 1986 - Engineering Notes, pp 349-352.

[12]Baker, J. P., van Dam, C.P., and Gilbert, B. L., "Flatback Airfoil Wind Tunnel Experiment," Sandia Report SAND2008-2008, April 2008.

[13]Berg, D. E., and Barone, M., "Aerodynamic and Aeroacoustic Properties of a Flatback Airfoil," *WINDPOWER 2008*, June, Houston, USA.

[14]Allen, H. J., and Vincenti, W. G., "Wall Interference in a Two-Dimensional-Flow Wind Tunnel, with Consideration of compressibility," NACA Rept. 782, 1944.

[15]Ayuso, L., Sant, R., and Meseguer, J., "Aerodynamic Study of Airfoils with Leading Edge Imperfections at Low Reynolds Number," *AIAA 40th Fluid Dynamics Conference and Exhibit*, Chicago, Illinois, AIAA 2010-4625.